Thin Solid Films xxx (2016) xxx–xxx

Contents lists available at ScienceDirect

Thin Solid Films

journal homepage: www.elsevier.com/locate/tsf

Viscoelastic mechanical properties measurement of thin Al and Al–Mg films using bulge testing

An-Wen Huang [a,c], Cheng-Hua Lu [a], Shao-Chi Wu [a], Tzu-Ching Chen [b], Richard P. Vinci [c], Walter L. Brown [c], Ming-Tzer Lin [a,*]

[a] Graduate Institute of Precision Engineering, National Chung Hsing University, Taichung 402, Taiwan
[b] Chaoyang University of Technology, Taichung 413, Taiwan
[c] Department of Materials Science and Engineering, Lehigh University, Bethlehem, PA 18015, USA

ARTICLE INFO

Article history:
Received 17 November 2015
Received in revised form 30 March 2016
Accepted 30 March 2016
Available online xxxx

Keywords:
Aluminum alloy
Magnesium alloy
Thin films
Stress measurement
Temperature
Mechanical properties tests
Time-dependent response
Elastic modulus

ABSTRACT

Metal thin films are used as major components in microelectromechanical systems (MEMS). However, problems with long-term reliability that set limits on the lifetime of MEMS applications have been observed. The more efficiently the thin films resist stress relaxation, the longer the lifetime of the MEMS device. In particular, Al thin films have been used as capacitance switches, but are shown to have a low resistance to stress relaxation, thus hindering overall performance and leading to shorter lifetime. Using bulge testing, this study investigates the viscoelastic behavior of pure Al thin film in comparison with thin Al alloy films with 12% and 16% Mg. The results show that the addition of Mg to Al films significantly decreases the relaxation behavior and increases the strengthening mechanism of such thin films. The greater the Mg content in an Al film, the greater the resistance of the film. The normalized modulus decreases less with a greater Mg content. Al–Mg thin films have better relaxation resistance than pure Al thin films and thus serve as a better material for MEMS capacitance switches.

1. Introduction

Time and temperature dependent mechanical behavior is a known issue in relation to the reliability of MEMS (microelectromechanical ystem) devices, which are easily affected by creep, especially in high stress and high temperature environments [1]. It has been shown that thin metal films exhibit significantly recoverable time-dependent stress relaxation (viscoelasticity) than their bulk counterparts, even at very small strains, as evidenced by differences in the derived activation energy of the relaxation mechanisms [2–6]. The mechanical stability of thin metal films in MEMS devices is critical to consistent performance, the reason why this issue is important.

For instance, in an RF MEMS capacitive switch, thin metal-on-dielectric contact layers separate the stationary and moving electrodes on closure to prevent a DC short circuit, actuating voltage from the RF switch to the adjacent stationary electrode [7,8]. However, if the RF switch has been used repeatedly, an electrical charge can accumulate in the dielectric layer [9–11]. As a consequence, the stored elastic energy in the membrane may be too small to oppose the electrostatic force, and the switch will fail to close. If there is also relaxation in the stress of the deflected membrane over time, the tendency to fail to close will increase, even if the stored dielectric charge remains constant.

Low-melting metal thin films, *e.g.* Al, are sensitive to creep and viscoelastic behavior. However, as many of the movable bridges in RF MEMS switches are fabricated from Al [12], it is important to increase the creep resistance of the Al thin films. Hyun et al. [13] previously studied the stress relaxation of Al thin films and found that creep resistance increased in relation to the increase in the thickness of the film, reporting that the reduction in the relaxation rate relative to the increase in thickness was due to the dislocation locking mechanism.

In bulk metals, creep resistance can be enhanced by the introduction of other atoms into the solid matrix at high temperatures to strengthen the material. Firstly, the solid solution is supersaturated during the heating process. After cooling, the excess solute precipitates. This precipitate creates an effective obstacle to the dislocation motion [14] and strongly enhances the creep resistance of bulk Al. However, in a microelectronic or MEMS application, the thermal process used in bulk metals is limited for the metals' thin film counterparts. Therefore, the method used to strengthen bulk materials can be inappropriate for thin metal films.

This study uses a different approach for a strengthening mechanism for Al and Al alloy thin films by co-sputtering with Mg and Al. The goal was to add Mg atoms to pure Al films and observe the differences in the creep resistant mechanism of Al alloy thin films, examining the time and

* Corresponding author.
E-mail address: mingtlin@nchu.edu.tw (M.-T. Lin).

http://dx.doi.org/10.1016/j.tsf.2016.03.064
0040-6090/

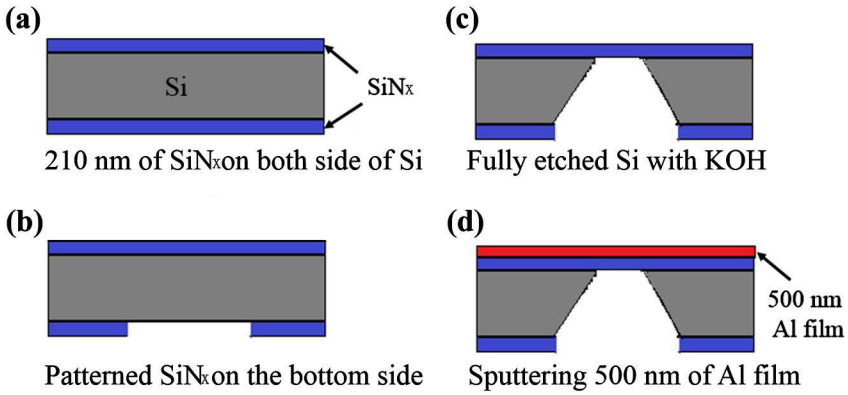

Fig. 1. The sequence of the fabrication process.

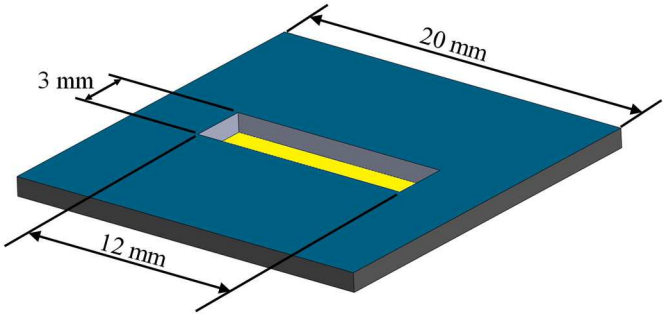

Fig. 2. Schematic view of the sample.

temperature dependent viscoelastic stress relaxations. The consequences of this strengthening behavior for MEMS capacitive switches are discussed below.

2. Experiments

Stress relaxation experiments were conducted on 500 nm thick Al and Al–Mg films using gas pressure bulge testing [15]. Fig. 1 shows the standard semiconductor fabrication methods used to make the bulge. The thin film membrane was made with a 20 mm by 20 mm silicon die which had a window, 12 mm long and 3 mm wide, in the center, as shown in Fig. 2. Each silicon die was coated with 210 nm SiNx on both sides, with the SiNx on the reverse side made using the photolithography method. The silicon dies were immersed in 45% (weight percent) KOH at a temperature of 85° until the silicon was fully etched. The Al and Al–Mg thin films were then deposited by DC magnetron sputtering onto the silicon nitride-coated fully etched silicon dies. All the thin films were created by DC magnetron sputtering using a system obtained from AJA international (ATC 2200 sputtering system). For the Al–Mg alloy films, a dual gun co-sputtering configuration was used.

The bulge system, shown in Fig. 3, has two chambers. One is the vacuum chamber and the other is the bulge chamber. N_2 gas was used to pressurize one side of the membrane, while the other side was kept under vacuum. The pressure was measured and controlled with a diaphragm manometer and controller. The bulge height was continually measured as a function of time. The height was dependent on the capacitance between the metal membrane and a 6-mm × 6-mm capacitor plate held at a fixed distance of approximately 150 μm from the surface of the window frame around the membrane, as shown in Fig. 3. The size of the plate has to be wide enough so that the capacitance is insensitive to precise placement over the 3-mm window width and short enough so that it only measures the central 6 mm of the bulge, avoiding the non-cylindrical ends. The strain is determined from the radius of the cylindrical bulge, R, which is deduced from the capacitance as

$$\mathbf{C} = 4\varepsilon_0 \mathbf{b} \frac{\sqrt{4\mathbf{R}^2 - \mathbf{D}^2}\cdot \arctan\left(\frac{\mathbf{D}}{\sqrt{4\mathbf{B}\sqrt{4\mathbf{R}^2 - \mathbf{D}^2} - \mathbf{D}^2}}\right)}{\sqrt{4\mathbf{B}\sqrt{4\mathbf{R}^2 - \mathbf{D}^2} - \mathbf{D}^2}} \tag{1}$$

where b is the length of the capacitor plate, D is the width of the window, and B is the distance between the un-bulged film and the capacitor plate. The pressure difference created an approximately cylindrical bulge in the membrane, the radius of which was determined by measuring the change in capacitance $\boldsymbol{C}$ between the membrane and a fixed electrode. This radius R, along with the applied pressure p, was used to calculate both the stress σ and strain ε in the membrane in the hoop direction (along the shorter axis) using the following equations:

$$\sigma = \frac{\mathbf{P}\cdot\mathbf{R}}{\mathbf{t}} \tag{2}$$

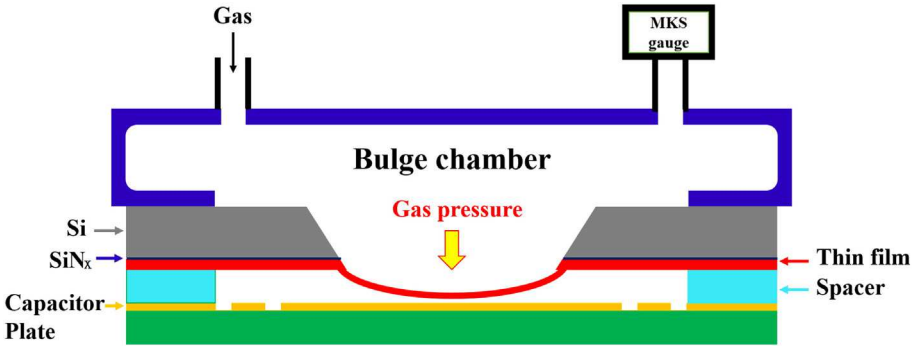

Fig. 3. Schematic of the measuring system.

Please cite this article as: A.-W. Huang, et al., Viscoelastic mechanical properties measurement of thin Al and Al–Mg films using bulge testing, Thin Solid Films (2016), http://dx.doi.org/10.1016/j.tsf.2016.03.064

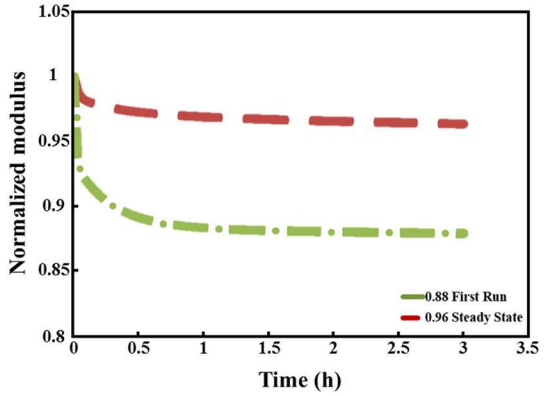

Fig. 4. Initial and steady state viscoelastic relaxation behavior tested at room temperature.

$$\varepsilon = \frac{l - D}{D} = \frac{2R \cdot \arcsin\left(\frac{D}{2R}\right) - D}{D} \tag{3}$$

where t is the film thickness (500 nm) and D is the membrane width (3 mm). Because the aspect ratio of the membrane was 4:1, it was assumed that the applied strain along the length of the membrane was essentially zero (plane strain condition) [16]. The applied pressure was controlled by a MKS pressure controller under the command of a computer running the Labview program. The gas pressure creates a pressure difference between both sides of the film and a bulge in the thin membrane. The experimental setup also allowed for the control of temperature that is independent of the stress, a feature unavailable in many other forms of thin-film mechanical testing.

Mechanical testing of pressure cycles and stress relaxations at constant applied strain were performed. Tests were conducted at temperatures of 293, 323, 343, and 353 K indicating the typical operating temperatures of a MEMS switch. With regards to the pressure cycle experiment, the applied pressure was increased from zero until a preset maximum was reached at a rate of 533.3 Pa/s. This corresponded to a strain rate of approximately 10^{-4}/s. The pressure was then returned to zero at the same rate, giving elastic stiffness and average residual stress. The elastic stiffness measured here was the plane strain modulus $M = E/(1-\nu^2)$, defined as the slope of the unloading segment of the stress–strain curve [16]. The average residual stress for the film was determined from the unloading segment of the stress–strain curve to a strain value of zero. Since the SiNx is retained beneath the Al or Al–Mg thin films, all thin films were measured as composite films. The pressure cycle experiments for the sole SiNx film were performed prior to the actual Al/SiNx or Al–Mg/SiNx composite film experiments.

Table 1
The temperature dependence of SiNx properties.

Temperature	Initial stress (MPa)	Modulus (GPa)
297 K	424.2	225.4
323 K	453.1	226.4
343 K	427.1	227.0
353 K	481.7	227.3

Knowing the properties of SiNx, the plane strain modulus and average residual stress of Al and Al–Mg films can thus be ascertained by

$$\sigma_{composite} = \frac{\sigma_{Al} t_{Al} + \sigma_{SiN_x} t_{SiN_x}}{t_{Al} + t_{SiN}} \tag{4}$$

$$M_{composite} = \frac{M_{Al} t_{Al} + M_{SiN_x} t_{SiN_x}}{t_{Al} + t_{SiN_x}} \tag{5}$$

where M is the plane strain modulus, σ is stress and t is the thickness.

In the stress relaxation experiment, the pressure was increased until the applied strain of the membrane reached a value of 1×10^{-3}. A feedback loop was then performed which controlled the applied pressure and maintained a constant applied strain. The test condition was held for 3 h before the pressure was returned to zero.

3. Results and discussion

It has previously been shown that it is necessary to run a metal film through cyclic relaxation cycles before a fully viscoelastic state is reached [17,18]. Once steady viscoelasticity has been attained, there is no further viscoplastic contribution to the relaxation. Thus, the total amount of relaxation that occurs during the steady state test is less than during the first cycle. As shown in Fig. 4, any further relaxation cycles would result in identical results to the second test depicted here. Once the film portrayed in Fig. 4 reached its steady-state condition, the Al and Al–Mg films were then subjected to three-hour long relaxation experiments at room temperature, with a pressure cycle prior to each, before any tests at elevated temperatures were conducted.

Fig. 5 shows the results from the first pressure cycle experiment for the Al/SiNx thin films at room temperature (293 K). For a purely elastic material, the loading and unloading segments should overlap. As intended, there was no sign of classic plasticity, evident from a distinct change in the loading slope at the onset of the plastic yielding. The two halves of the stress/strain plot are both straight lines with a similar slope. The slope of the unloading line gives a value for the elastic modulus. Since the thicknesses of Al and SiNx are 500 nm and 210 nm, respectively, the plane strain modulus of Al from Eq. (5) can

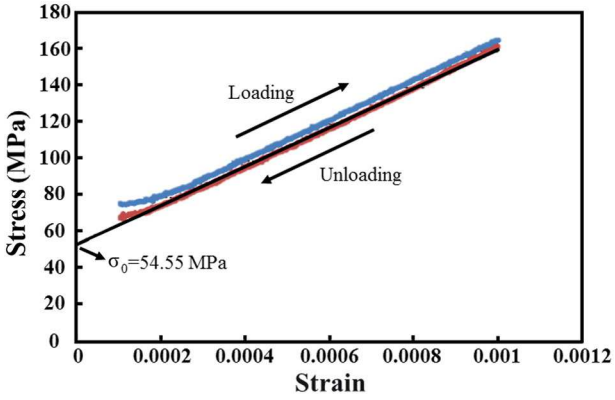

Fig. 5. Stress strain results from the first pressure cycle experiment of the Al/SiNx thin films at room temperature.

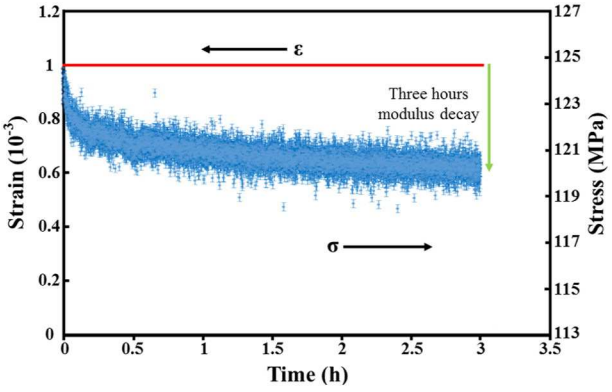

Fig. 6. Steady state stress relaxation experiment for pure Al/SiNx film conducted at room temperature at constant strain.

be obtained. The interception of the unloading line on the stress axis is the residual stress in the film at zero strain.

Table 1 summarizes the average residual stress and the plane strain modulus of SiNx from previous pressure ramp experiments under 293, 323, 343 and 353 K. It is clear that silicon nitride film is temperature independent, with a plane strain modulus of approximately 226 GPa. These values were used in the calculation to obtain the actual test values for Al and Al–Mg thin films.

The steady state stress relaxation at a constant strain over a period of 3 h is shown in Fig. 6. There is a step change in the applied strain from zero to 1×10^{-3} at $t = 0$. After that, the strain is automatically maintained at a constant value. At the strain step, the stress rises to a peak of 125 MPa and then relaxes over the 3-hour period to about 80 MPa. Therefore, time dependence can be expressed as a time-dependent elastic relaxation modulus M(t), also called an effective modulus, by

$$\mathbf{M(t)} = \frac{\boldsymbol{\sigma}(\mathbf{t}) - \boldsymbol{\sigma}_0}{\boldsymbol{\varepsilon}(\mathbf{t})} \tag{6}$$

where ε is the value of the constant strain maintained throughout the 3 h. The results from the relaxation modulus were then normalized and defined as the initial modulus divided by the time, which is given by $N.M(t) = M(t)/M_0$, in which N.M(t) is the normalized modulus. Fig. 6 shows the results obtained from the steady state relaxation experiment for pure Al/SiNx film conducted at room temperature. Plotted in this graph is the normalized effective modulus during the 3-hour relaxation. As defined in this study, the effective modulus is identical to the relaxation modulus, typically defined in the stress relaxation experiments on polymers [19]. The normalized effective modulus $M(t)/M_0$ is simply the effective modulus at a given time divided by the initial effective modulus, representing the fraction of the initial modulus that remains as a function of time. The data shown in Fig. 6 indicate that the reduced modulus decreased to a value of 0.96 of its start value, corresponding to a 4% decay. Also shown in Fig. 7 is a Prony series fit for the relaxation data. A Prony series is commonly used to mathematically describe linear viscoelastic behavior and has the form

$$\mathbf{N.M(t)} = 1 - \sum_{\mathbf{i}=1}^{\mathbf{N}} \mathbf{P_i}\left(1 - \mathbf{e}^{\frac{-\mathbf{t}}{\tau_i}}\right) \tag{7}$$

where N is the normalized factor, M(t) is the modulus at a given time, P_i is the i_th strength coefficient, and τ_i is the i_th time constant. In this paper, a four-term fit was used ($n = 4$), with four pairs of strength coefficients and time constants generated. To ensure that the fit was representative of the data from all time ranges, the time constants were fixed at one per decade (10, 100, 1000, and 10,000 s) [17,18]. To reveal any elevated temperature exposure effects on subsequent relaxations at lower temperatures, additional tests were conducted at 343, 323, and 293 K. Fig. 8a shows the Prony series fits for the results obtained in the decreasing temperature experiments.

Next, a series of stress relaxation experiments for different Mg contents in Al thin films were conducted as a comparison to the pure Al results. It should be noted that all the relaxation tests for both Al and Al–Mg followed the same procedures, with only the steady state relaxations observed in comparisons between the films. Fig. 8b shows the time and temperature dependencies of the 3-hour normalized modulus fitted with the Prony series for the 12.4% Mg–Al alloy films in the same y-scale.

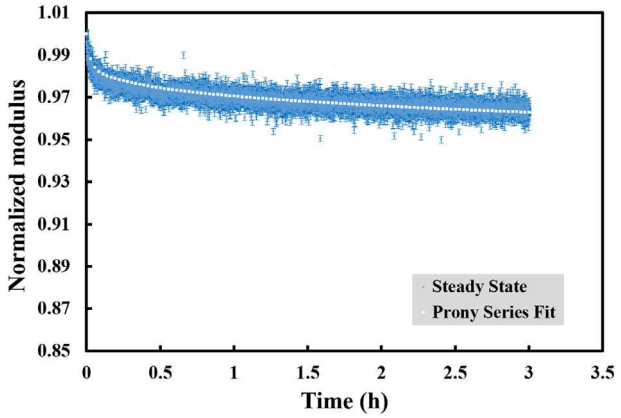

Fig. 7. A Prony series fit for the stress relaxation data tested in Fig. 6.

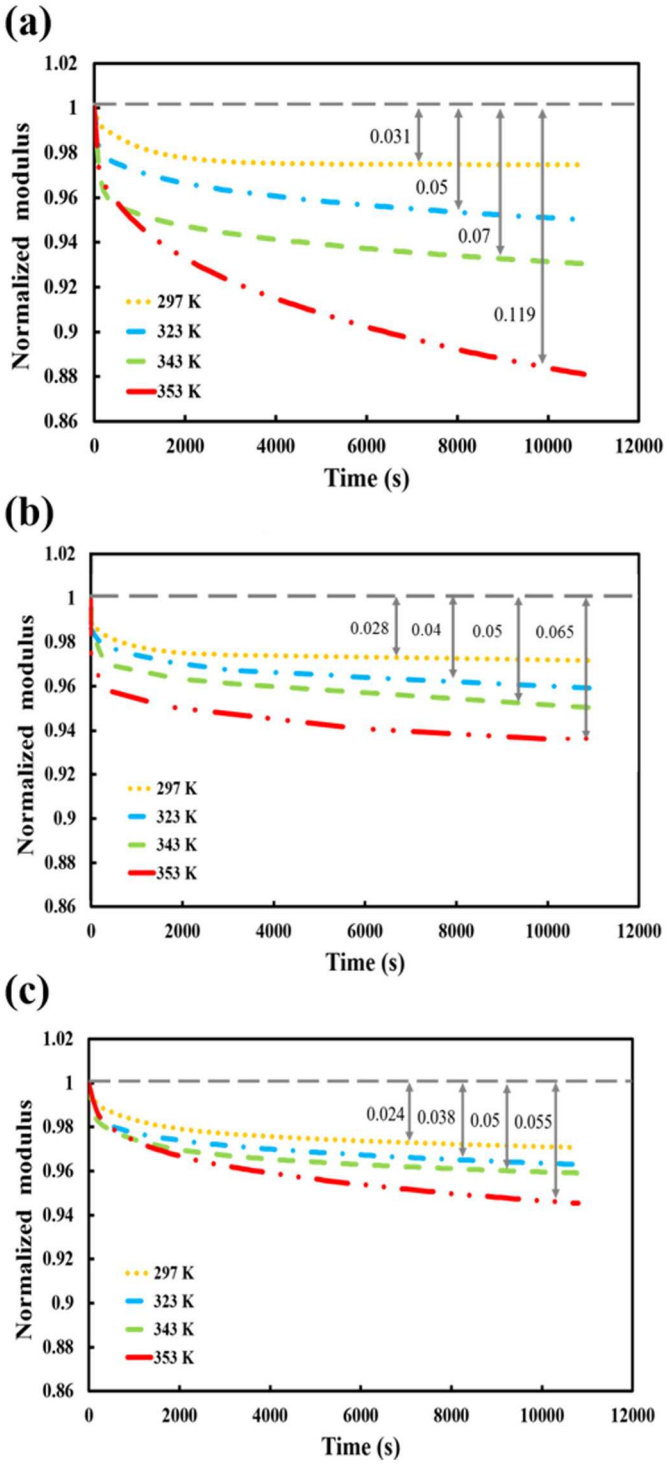

Fig. 8. Three-hour modulus decay of pure and Mg containing Al thin films with the prony series fit at each temperature (a) 0% Mg (b) 12.38% Mg (c) 16.30%.

Please cite this article as: A.-W. Huang, et al., Viscoelastic mechanical properties measurement of thin Al and Al–Mg films using bulge testing, Thin Solid Films (2016), http://dx.doi.org/10.1016/j.tsf.2016.03.064

Table 2
Prony series constants of pure Al, 12.38% Mg, and 16.30% Mg at different temperatures.

Temperature		P_1(10 s)	P_2(100 s)	P_3(1000 s)	P_4(10000 s)
297 K	Pure Al thin film	0.00306	0.00311	0.004925	0.00833
	12.38%Mg thin film	0.000994	0.010411	0.007953	0.022573
	16.30%Mg thin film	0.004682	0.012132	0.005211	0.047142
323 K	Pure Al thin film	0.004769	0.00422	0.005539	0.009335
	12.38%Mg thin film	0.000619	0.007616	0.003712	0.025624
	16.30%Mg thin film	0.007075	0.012041	0.01513	0.005696
343 K	Pure Al thin film	0.004853	0.005058	0.01003	0.03113
	12.38%Mg thin film	0.002174	0.006499	0.002984	0.026414
	16.30%Mg thin film	0.007235	0.002886	0.01514	0.06011
353 K	Pure Al thin film	0.005637	0.006244	0.024268	0.10118
	12.38%Mg thin film	0.004118	0.0060610	0.004712	0.030037
	16.30%Mg thin film	0.008517	0.0039801	0.018038	0.072157

Fig. 8c shows the time and temperature dependencies of the 3-hour normalized modulus fitted with the Prony series for the 16.3% Mg Al alloy films in the same y-scale. Table 2 lists the Prony series coefficient values for the fits at all steady-state conditions in chronological order.

For all plots, the normalized modulus decreases with increases in temperature. The values of the 3-hour normalized modulus decays are shown in Table 3, showing that increasing amounts of Mg to Al thin films (up to 16%) demonstrate lower relaxation decay. When comparing the 3-hour modulus decay between pure Al and Al–Mg thin films over the 293–353 K temperatures, pure Al varies from 3.1% to 11.9%. Meanwhile, the 12.63% Mg content in the Al–Mg alloy varies from 2.8% to 6.5%, and the 16.30% Mg content in the Al–Mg alloy from 2.4% to 5.5%. In these data, relaxation processes play a role and their behavior is determined by the activation energies relative to kT. Taking Arrhenius plot of time constant versus 1/T, the activation energies of pure Al, 13% Mg Al, and 16% Mg Al thin films were calculated to be 6.50 kJ/mol, 16.80 kJ/mol and 20.30 kJ/mol, respectively.

It is apparent that Al–Mg specimens have increased resistance to viscoelastic relaxation compared to the pure Al specimens. This is most prominent where the alloyed specimens achieve stress levels that are substantially above those of the pure Al specimens before saturation.

A typical mechanical effect of a solute added to a pure bulk metal is to increase yield strength by pinning dislocations that are properly oriented with respect to certain solute atoms so as to induce attractive interactions between their respective strain fields. It appears, overwhelmingly, there is a similar effect for Al–Mg alloy thin films. Regardless of the magnitude of the solute–dislocation interaction, the effect on strength increases monotonically with the increase in solute concentration. At very low concentrations, the strength is generally proportional to $C^{1/2}$ [20]. At higher solute concentrations, a linear dependence on $C^{2/3}$ is often observed instead [21,22].

Fig. 9 presents the transmission electron microscopy (TEM) images of pure Al, 13% Mg Al, and 16% Mg Al films, respectively. These thin film samples were cut from FIB after the standard 3-hour stress relaxation tests were performed. The TEM images reveal a significant increase in grain size with thickness for all three 500-nm films, with the grain size of pure Al thin film substantially bigger than the alloy thin films. Grain growth in pure metal films is found to stagnate quickly after a certain annealing temperature is reached, often within seconds or minutes, so it is likely that the grain size reported here for pure Al represents a limiting grain size for these particular films [23]. It is often observed that the grain size in the plane of the film closely matches the film thickness itself. However, it is clear from Fig. 9 that the addition of Mg to Al results in a major reduction in grain size and it can be surmised that the Mg atoms interfere with normal Al grain growth by decreasing grain boundary mobility. With this simple picture, it is somewhat surprising that the grain size is essentially the same for all of the alloy samples. In a prior study of solid solution strengthening in Pt–Ru alloys, an almost linear inverse relationship was found between solute concentration and grain size after annealing [24].

Grain size stagnation in thin metal films is generally attributed to the drag effect induced by the intersection of the grain boundaries with the free surface(s). If impurities are present, an additional drag force, due to grain boundary segregation, will play a role. If the grain size varies with solute concentration, then it would seem reasonable to conclude that the equilibrium grain boundary solute concentration will also vary. Conversely, if the grain size is constant for a range of solute concentrations, one may argue that grain boundary solubility is low. Hence, the limiting grain boundary concentration would be reached at very low solute concentrations, with the remaining atoms retained in the bulk. As the grain size was not measured prior to tests and annealing, it is impossible to estimate how much of the final measured grain size was established during deposition and how much by grain growth during the annealing process. Therefore, grain size could have been determined by the increased tendency of the nucleation of new grains during deposition or by the inhibition of grain growth after deposition [25]. Nevertheless, one source of relaxation resistance can be attributed to the strengthening of the grain boundary, which is particularly significant when the grain size is small.

Table 3
Three hour normalized modulus decay of pure Al, 12.63% Mg, and 16.30% Mg at different temperatures.

Temperature	3 hour decay (%)		
	Al	12.63%Mg	16.30%Mg
297 K	3.1	2.8	2.4
323 K	5	4	3.8
343 K	7	5	5
353 K	11.9	6.5	5.5

4. Conclusion

This study demonstrated an approach to the measurement of the time- and temperature-dependent effective elastic modulus of 500 nm-thick Al and Al–Mg alloy thin films, as characterized during numerous stress relaxation cycles and over the temperature range of 293 – 353 K. A steady-state condition was established for the films in which all stress relaxation was fully recoverable. Furthermore, by increasing the temperature, both the strength and rate of relaxation increased, implying that the relaxation mechanism is temperature dependent. The viscoelastic behavior of pure Al thin film, in comparison with thin films of 12.63%Mg Al and16.30%Mg Al alloys, was also investigated. It was observed that the addition of Mg to Al thin films produces major changes in the grain structure and in the mechanical properties. Grain size is strongly reduced by the addition of Mg, and these films showed a marked increase in resistance to viscoelastic relaxation, both at room temperature (293 K) and higher temperatures up to 353 K. This may be seen as an attractive feature of this material system for certain applications, such as RF MEMS capacitive switches in the microelectronics industry.

Please cite this article as: A.-W. Huang, et al., Viscoelastic mechanical properties measurement of thin Al and Al–Mg films using bulge testing, Thin Solid Films (2016), http://dx.doi.org/10.1016/j.tsf.2016.03.064

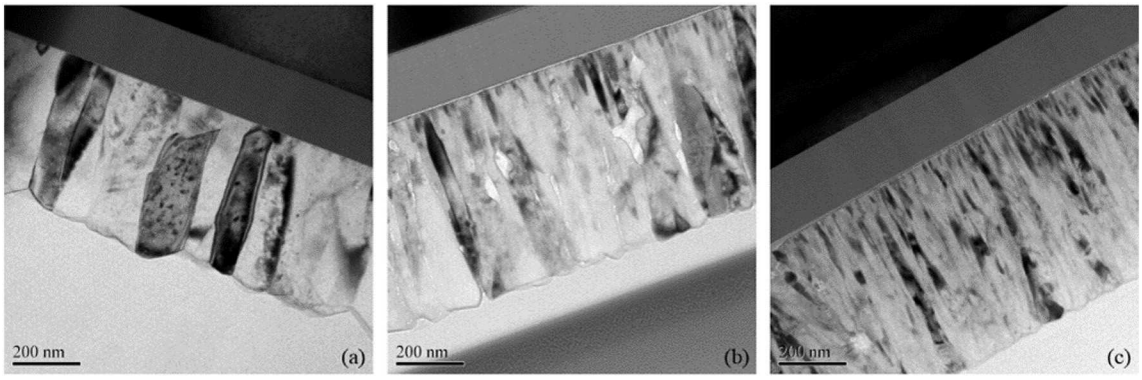

Fig. 9. The TEM picture of thin film (a) pure Al (b) 12.63% Mg (c) 16.30%.

Acknowledgements

This work was supported by the National Science Foundation (NSF) via award CMMI-1332574 and the Taiwan Ministry of Science and Technology under grant MOST 103-2221-E-005-008. This work was also supported in part by the Ministry of Education, Taiwan under the ATU plan.

References

[1] R. Modlinski, A. Witvrouw, P. Ratchev, R. Puers, J.M.J. Den Toonder, I. De Wolf, Creep characterization of Al alloy thin films for use in MEMS applications, Microelectron. Eng. 76 (1–4) (2004) 272–278.
[2] M. Hershkovitz, I.A. Blech, Y. Komem, Stress relaxation in thin aluminium films, Thin Solid Films 130 (1/2) (Aug. 1985) 87–93.
[3] R.P. Vinci, G. Cornella, J.C. Bravman, Anelastic contributions to the behavior of freestanding Al thin films, Proc. 5th Int. Workshop Stress Induced Phenom, Metallization, vol. 491 1999, pp. 240–248.
[4] H. Lee, G. Cornella, J.C. Bravman, Stress relaxation of freestanding aluminum beams for microelectromechanical systems applications, Appl. Phys. Lett. 76 (23) (Jun. 2000) 3415–3417.
[5] A.J. Kalkman, A.H. Verbruggen, G.C.A.M. Janssen, Young's modulus measurements and grain boundary sliding in free-standing thin metal films, Appl. Phys. Lett. 78 (18) (Apr. 2001) 2673–2675.
[6] P.A. Gruber, S. Olliges, E. Arzt, R. Spolenak, Temperature dependence of mechanical properties in ultrathin Au films with and without passivation, J. Mater. Res. 23 (9) (2008) 2406–2419.
[7] R.E. Strawser, K.D. Leedy, R. Cortez, J.L. Ebel, S.R. Dooley, C.F. Herrmann Abell, V.M. Bright, Influence of metal stress on RF MEMS capacitive switches, *Sensors Actuators A Phys.* 134 (2) (Mar. 2007) 600–605.
[8] C.L. Goldsmith, D. Forehand, Temperature variation of actuation voltage in capacitive MEMS switches, *IEEE Microwave Wireless Compon. Lett.* 15 (10) (Oct. 2005) 718–720.
[9] J.C.M. Hwang, Reliability of electrostatically actuated RF MEMS switches, Proc. IEEE Radio-Frequency Integration Technology (RFIT) Dec. 9–11, 2007, pp. 168–171.
[10] X. Yuan, Z. Peng, J.C.M. Hwang, D. Forehand, C.L. Goldsmith, A transient SPICE model for dielectric-charging effects in RF MEMS capacitive switches, *IEEE Trans. Electron Devices* 53 (10) (Oct. 2006) 2640–2648.
[11] Z. Peng, X. Yuan, J.C.M. Hwang, D. Forehand, C.L. Goldsmith, Superposition model for dielectric charging of RF MEMS capacitive switches under bipolar control-voltage waveforms, *IEEE Trans. Microwave Theory Tech.* 55 (12) (Dec. 2007) 2911–2918.
[12] R. Modliniski, P. Ratchev, A. Witvrouw, R. Puers, I. Do Wolf, Creep-resistant aluminum alloys for use in MEMS, J. Micromech. Microeng. 15 (2005) S165–S170.
[13] S. Hyun, W.L. Brown, R.P. Vinci, Thickness and temperature dependence of stress relaxation in nanoscale aluminum films, Appl. Phys. Lett. 83 (21) (2003) 4411–4413.
[14] W.D. Callister Jr., Material Science and Engineering, Wiley, New York, 1985 (chapter 7).
[15] J.J. Vlassak, W.D. Nix, A new bulge test technique for the determination of Young's modulus and Poisson's ratio of thin films, J. Mater. Res. 7 (12) (Dec. 1992) 3242–3249.
[16] Y. Xiang, X. Chen, J.J. Vlassak, Plane-strain bulge test for thin films, J. Mater. Res. 20 (9) (Sep. 2005) 2360–2370.
[17] X. Yan, W.L. Brown, Y. Li, J. Papapolymerou, C. Palego, J.C.M. Hwang, R.P. Vinci, Anelastic stress relaxation in gold films and its impact on restoring forces in MEMS devices, J. Microelectromech. Syst. 18 (3) (Jun. 2009) 570–576.
[18] M. McLean, W.L. Brown, R.P. Vinci, Temperature-dependent viscoelasticity in thin Au films and consequences for MEMS devices, J. Microelectromech. Syst. 19 (6) (2010) 1299–1308.
[19] I.M. Ward, D.W. Hadley, An Introduction to the Mechanical Properties of Solid Polymers, first ed. Wiley, Chichester, U.K., 1993
[20] R.L. Fleischer, Solution hardening, Acta Metall. 9 (1961) 996–1000.
[21] R.W. Cahn, P. Haasen (Eds.), Physical Metallurgy, North-Holland, 1996.
[22] R. Labusch, Phys. Status Solidi 41 (1970) 659.
[23] E.M. Zielinski, R.P. Vinci, J.C. Bravman, The influence of strain energy on abnormal grain growth in copper thin films, Appl. Phys. Lett. 67 (8) (1995) 1078.
[24] S. Hyun, R.P. Vinci, K.P. Fahey, B.M. Clemens, Effect of grain structure on the onset of diffusion-controlled relaxation in Pt thin films, Appl. Phys. Lett. 83 (14) (2003) 2769–2771.
[25] M.-T. Lin, R.R. Chromik, N. Barbosa, P. El-Deiry, S. Hyun, W.L. Brown, R.P. Vinci, T.J. Delph, The influence of vanadium alloying on the high-temperature mechanical properties of thin gold films, Thin Solid Films 515 (2007) 7919.

Please cite this article as: A.-W. Huang, et al., Viscoelastic mechanical properties measurement of thin Al and Al–Mg films using bulge testing, Thin Solid Films (2016), http://dx.doi.org/10.1016/j.tsf.2016.03.064